The Astrophysical Journal Letters, 854:L27 (7pp), 2018 February 20 https://doi.org/10.3847/2041-8213/aaacfd

2MASS J13243553+6358281 Is an Early T-type Planetary-mass Object in the AB Doradus Moving Group

Jonathan Gagné[1,6], Katelyn N. Allers[2], Christopher A. Theissen[3], Jacqueline K. Faherty[4], Daniella Bardalez Gagliuffi[4], and Étienne Artigau[5]
[1] Carnegie Institution of Washington DTM, 5241 Broad Branch Road NW, Washington, DC 20015, USA; jgagne@carnegiescience.edu
[2] Department of Physics and Astronomy, Bucknell University, Lewisburg, PA 17837, USA
[3] Center for Astrophysics and Space Sciences, University of California, San Diego, 9500 Gilman Drive, Mail Code 0424, La Jolla, CA 92093, USA
[4] Department of Astrophysics, American Museum of Natural History, Central Park West at 79th Street, New York, NY 10024, USA
[5] Institute for Research on Exoplanets, Université de Montréal, Département de Physique, C.P. 6128 Succ. Centre-ville, Montréal, QC H3C 3J7, Canada
Received 2018 January 28; revised 2018 January 31; accepted 2018 February 1; published 2018 February 16

Abstract

We present new radial velocity and trigonometric distance measurements indicating that the unusually red and photometrically variable T2 dwarf 2MASS J13243553+6358281 is a member of the young (∼150 Myr) AB Doradus moving group (ABDMG) based on its space velocity. We estimate its model-dependent mass in the range 11–12 $M_{\rm Jup}$ at the age of the ABDMG, and its trigonometric distance of 12.7 ± 1.5 pc makes it one of the nearest known isolated planetary-mass objects. The unusually red continuum of 2MASS J13243553+6358281 in the near-infrared was previously suspected to be caused by an unresolved L + T brown dwarf binary, although it was never observed with high spatial resolution imaging. This new evidence of youth suggests that a low surface gravity may be sufficient to explain this peculiar feature. Using the new parallax we find that its absolute *J*-band magnitude is ∼0.4 mag fainter than equivalent-type field brown dwarfs, suggesting that the binary hypothesis is unlikely. The fundamental properties of 2MASS J13243553+6358281 follow the spectral type sequence of other known high-likelihood members of the ABDMG. The effective temperature of 2MASS J13243553+6358281 provides the first precise constraint on the L/T transition at a known young age and indicates that it happens at a temperature of ∼1150 K at ∼150 Myr, compared to ∼1250 K for field brown dwarfs.

Key words: brown dwarfs – methods: data analysis – proper motions – stars: individual (2MASS J13243553 +6358281) – stars: kinematics and dynamics

Supporting material: data behind figure

1. Introduction

The recent discovery of isolated planetary-mass objects (e.g., Liu et al. 2013; Gagné et al. 2015a, 2017; Kellogg et al. 2016; Schneider et al. 2016b) and widely separated planetary-mass companions (Chauvin et al. 2005; Naud et al. 2014; Gauza et al. 2015) in a range of ages provides a picture of how the atmospheres of planetary-mass objects evolve with time. The absence of a much brighter host star in their vicinity makes it possible to obtain high-resolution and high signal-to-noise spectra of their atmospheres with currently available facilities. These data are providing the foundations for our interpretation of the atmospheric features of directly imaged gas giant exoplanets such as 51 Eri b (Macintosh et al. 2015). Recent work has demonstrated overall similarities between such planetary-mass objects and giant planets at similar temperatures in their atmospheric features, but also significant differences caused mainly by their lower surface gravities. These include an excess flux in the *K* band caused by weakened collision-induced absorption of the H_2 molecule, compounded by a redder continuum slope at near-infrared wavelengths caused by thicker clouds (e.g., see Allers & Liu 2013; Gagné et al. 2015b; Faherty et al. 2016). Recent work has also indicated tentative evidence that there may exist a correlation between low surface gravity and the presence of high-amplitude photometric variability (Metchev et al. 2015; Biller et al. 2018; Gagné et al. 2017; Naud et al. 2017), but the small sample size still prevents a solid confirmation of this trend.

Because substellar objects cool down as they age (Burrows et al. 2001), one of the main strategies to identify planetary-mass objects has been to focus on young associations with a well-known age, which provides a way to estimate masses based on observed temperatures and evolutionary models. The nearest young associations have a few members within 10 pc of the Sun (e.g., Gagné et al. 2017), making them compelling laboratories to identify the lowest-mass objects in magnitude-limited surveys. However, their proximity means that their members are spread on large areas of the sky, making it hard to identify new members at a high confidence without measuring their full six-dimensional kinematics. This includes the *XYZ* Galactic coordinates and *UVW* space velocity, which require measurements of the trigonometric parallax and radial velocity. Several methods were introduced to identify the most promising candidate members of young associations before measuring their radial velocity and distance (e.g., Malo et al. 2013; Gagné et al. 2014; Riedel et al. 2017; Shkolnik et al. 2017), but all of them suffer from relatively low recovery rates and high rates of contamination for the nearest associations.

A new Bayesian tool, BANYAN Σ (Gagné et al. 2018), was recently built to identify members of young associations, with an updated method and new kinematic models for the associations based on the first data release of the *Gaia* mission (Lindegren et al. 2016) that provided 2 million parallaxes for nearby bright stars. This tool served as the base to start the BASS-Ultracool survey (J. Gagné et al. 2018, in preparation; see also Gagné

[6] NASA Sagan Fellow.

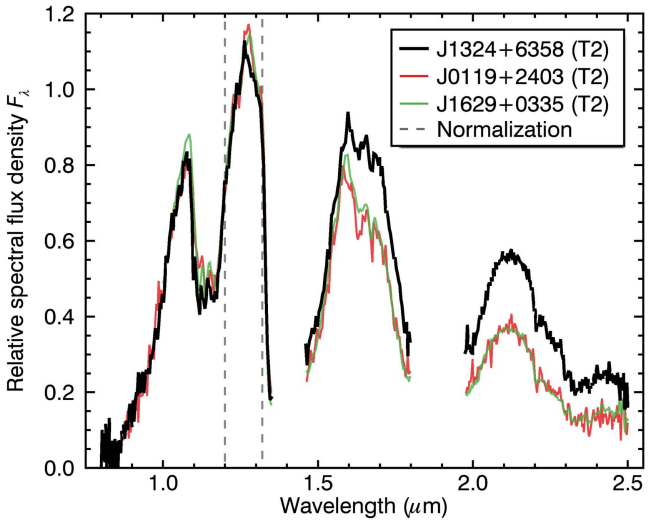

Figure 1. Relative spectral energy distribution of 2MASS J1324+6358 compared with two field T2 dwarfs. 2MASS J1324+6358 has a much redder slope, which was previously identified as a sign of either a young age or an unresolved L9 + T2 binary.

et al. 2015a, 2017; Bardalez Gagliuffi et al. 2018), an all-sky search for isolated planetary-mass objects in 2MASS (Skrutskie et al. 2006) and AllWISE (Wright et al. 2010; Kirkpatrick et al. 2014), with a particular focus on objects in the T spectral class where clouds migrate to depths below their photosphere and methane becomes apparent in their spectra (Burgasser et al. 2006). As part of this work, the known substellar object 2MASS J13243553+6358281 (2MASS J1324+6358 hereafter) was identified as a candidate member of the 149^{+51}_{-19} Myr old (Bell et al. 2015) AB Doradus moving group (ABDMG; Zuckerman et al. 2004), based on its sky position and proper motion only.

Here, we report the first measurements of a trigonometric distance and radial velocity based respectively on data from the *WISE* survey and a new mid-resolution GNIRS spectrum, which indicate that 2MASS J1324+6358 has kinematics consistent with the locus of ABDMG members. This is a strong indication that it is a young, low-gravity T dwarf in ABDMG and makes it unnecessary to invoke binarity to explain its peculiar spectroscopic features. We review relevant literature data on 2MASS J1324+6358 in Section 2. In Section 3, we detail the new GNIRS spectrum that was used to measure its radial velocity. The kinematics of 2MASS J1324+6358 are measured using these new data and *WISE* astrometry in Section 4, where its membership to ABDMG is also detailed. The fundamental properties of 2MASS J1324+6358 are discussed in Section 5, and this work is concluded in Section 6.

2. Literature Data

2MASS J1324+6358 was identified as a substellar object by Looper et al. (2007) and was noted for its unusually red slope in the near-infrared (see Figure 1). It was hypothesized that the most likely causes of this peculiar feature were either that this object has a very young age (estimated at <300 Myr) or that it consists of an unresolved binary with spectral types estimated at L9 + T2. Metchev et al. (2008) independently discovered this object and noted that its [4.5 μm]−[5.8 μm] IRAC color is redder than any known T dwarf. Burgasser et al. (2010) also posited that its peculiar spectral features may be due to binarity, but they noted that it was best fit by combining a T2 dwarf with 2MASS J10430758+2225236 (Cruz et al. 2007), one of the reddest known objects classified as an optical L8 dwarf. No high angular resolution imaging has been obtained yet for 2MASS J1324+6358.

Gagné et al. (2014) previously led an investigation of the potential young moving group membership of unusually red brown dwarfs with the BANYAN II Bayesian classifier and only obtained a 2.4% probability that 2MASS J1324+6358 is a member of ABDMG. However, they used near-infrared color–magnitude diagrams that were extrapolated at spectral types >L7 because late-type young objects were unknown at the time, and they indicated that their results should be interpreted with care at these late spectral types. These color–magnitude diagrams were responsible for missing 2MASS J1324+6358 as a candidate member of ABDMG, as ignoring them yields a 84% membership with BANYAN II using sky position and proper motion.

3. Observations

An intermediate-resolution near-infrared spectrum was obtained for 2MASS J1324+6358 in good weather conditions with the GNIRS spectrograph (Elias et al. 2006) at the Gemini-North telescope on UT 2018 January 5. Order 3 of the 110.5 l/mm grating with a central wavelength setting of 2.3 μm was used with the 0.″05/pix long camera and the 0.″15 slit, yielding a resolving power $\lambda/\Delta\lambda \sim 14{,}000$ over 2.27–2.33 μm. The target was nodded along the slit in a 6″-wide ABBA pattern for 13 exposures of 600 s each, yielding a median signal-to-noise ratio per pixel of ∼40. Standard calibrations consisting of six 20 s flat-field exposures and two 80 s Xe, Ar arc lamps were also obtained to correct pixel sensitivity and obtain an initial wavelength solution.

The data were reduced using a modified version of `REDSPEC`, Keck Observatory's facility data reduction package for high-resolution, near-infrared spectra. The reduction included an initial wavelength calibration (using sky emission lines as well as Xe, Ar arc lamps), flat-fielding and bad-pixel masking. Each nod pair was subtracted to eliminate sky emission, and the resulting A–B images were spatially and spectrally rectified. Spectra were extracted from these A–B images using an aperture equal to 0.67 times the FWHM of the seeing and subtracting residual sky lines using background windows without significant source flux. Uncertainties were calculated by propagating Poisson noise throughout the reduction process. The extracted spectra were combined using a robust weighted mean with the `xcombspec` procedure from the `Spextool` package (Cushing et al. 2004).

4. Kinematics

4.1. Radial Velocity

A forward model for the GNIRS spectrum was built from radial velocity-shifted BT-Settl (CIFIST) atmosphere models (Allard et al. 2012) convolved with a rotational broadening profile, including a second-degree polynomial wavelength solution. The `atran` model for MaunaKea (Lord 1992)[7] was

[7] Calculated at a zenith angle of 48° with 3.1 mm of water vapor, see https://atran.sofia.usra.edu/cgi-bin/atran/atran.cgi.

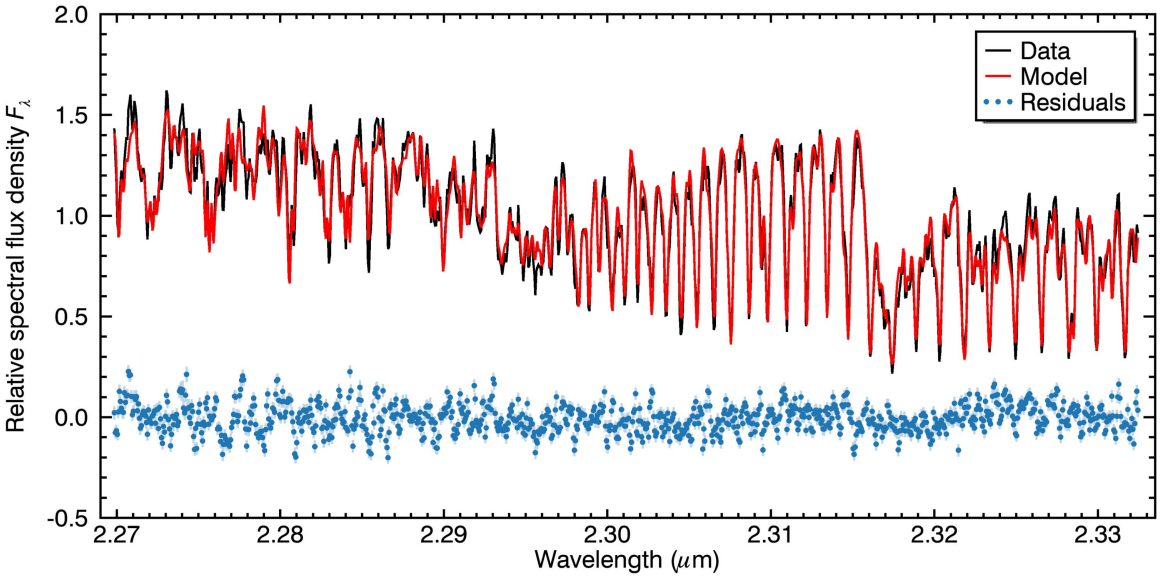

Figure 2. Best-fitting forward model (red) compared to the GNIRS spectrum of 2MASS J1324+6358 obtained here (black). Residuals are shown as blue dots. We obtain a reduced $\chi^2 = 2.3$. (The data used to create this figure are available.)

then included with optical depth as a free parameter to model telluric absorption, and the resulting spectrum was convolved with a Gaussian line spread function to represent instrumental effects. The best-fitting values for these seven forward model parameters were explored with a DREAM-ZS Markov Chain Monte Carlo method (ter Braak & Vrugt 2008), where values of $\log g$ and $T_{\rm eff}$ between grid points are explored by interpolating the nearest BT-Settl models on the grid. The corresponding Markov chains were used to build the probability density functions of the radial velocity and projected rotational velocity. A 4% systematic uncertainty was included in the data before performing this analysis so that the median uncertainties of the data match the median absolute residuals of the best fit. This resulted in a radial velocity of $-23.7^{+0.4}_{-0.2}$ km s^{-1} and a projected rotational velocity of $v \sin i = 11.5^{+1.0}_{-0.8}$ km s^{-1}. The model $\log g$ and $T_{\rm eff}$ values obtained from this forward fitting are $5.30^{+0.02}_{-0.01}$ dex and $1304.0^{+1.7}_{-1.5}$ K, respectively; however, such measurements for substellar objects based on fitting atmosphere models are unreliable especially when obtained from a narrow wavelength range (Filippazzo et al. 2015; Gagné et al. 2015b; Allers et al. 2016). This method is described in detail in Allers et al. (2016), where it is used to derive the radial velocity and projected rotational velocity of PSO J318.5–22 from a GNIRS spectrum obtained in the same configuration. The resulting best-fitting model is presented in Figure 2.

4.2. Trigonometric Distance

The trigonometric distance of 2MASS J1324+6358 was measured with a slight adaptation of the method described by Theissen (2017). In summary, all individual astrometric epochs of 2MASS J1324+6358 in the *W*1 and *W*2 bands were collected from all phases of the *WISE* mission[8] (providing a total baseline of 6.5 years) and compared to a parallax and proper motion solution with the Markov Chain Monte Carlo Python package `emcee` (Foreman-Mackey et al. 2013). The method of Theissen (2017) has only three free parameters corresponding to the parallax and the two dimensions of proper motion and compares the forward parallax model to all eight astrometric epochs relative to the first measurement. To avoid propagating the information of the first measurement across all epochs, we included the average sky position of 2MASS J1324+6358 as two additional free parameters. This modification makes this analysis less vulnerable to outlier measurements and yields more conservative error bars on all parameters. The resulting parallax measurement is 78.7 ± 9.0 mas, with a proper motion of $\mu_\alpha \cos\delta = -378.3 \pm 10.4$ mas yr^{-1} and $\mu_\delta = -68.0 \pm 5.7$ mas yr^{-1}. The best-fitting astrometric solution is displayed in Figure 3. As explained by Theissen (2017), this astrometric solution does not include a correction for the motion of background stars. They estimated a parallax correction of the order of 2 mas, well within the error bar for the parallax, but not for the proper motion, and we therefore adopt the proper motion measurement of Schneider et al. (2016a; based on 2MASS and AllWISE with a 10.4 year baseline), which is reported in Table 1 with our parallax measurement.

4.3. Kinematic Membership to Nearby Young Associations

The BANYAN Σ algorithm was used to determine the Bayesian probability that 2MASS J1324+6358 is a member of young associations within 150 pc of the Sun. The sky position, proper motion, radial velocity, and trigonometric distance of 2MASS J1324+6358 (see Table 1) were used and yielded an ABDMG membership probability of 98.0%. The measured *UVW* space velocity of 2MASS J1324+6358 (see Table 1) is located within 1.1 km s^{-1} of the locus of ABDMG members compiled in Gagné et al. (2018), within the velocity dispersion of the moving group (1.4 km s^{-1}), corresponding to a 0.7σ distance in the kinematics tri-dimensional space when accounting for the covariances in the distribution of existing ABDMG members. The Galactic coordinates *XYZ* of 2MASS J1324+6358 are located at ∼22.7 pc from the core

[8] *WISE* All-Sky, *WISE* 3-Band Cryo, *WISE* Post-Cryo, and NEOWISE Reactivation.

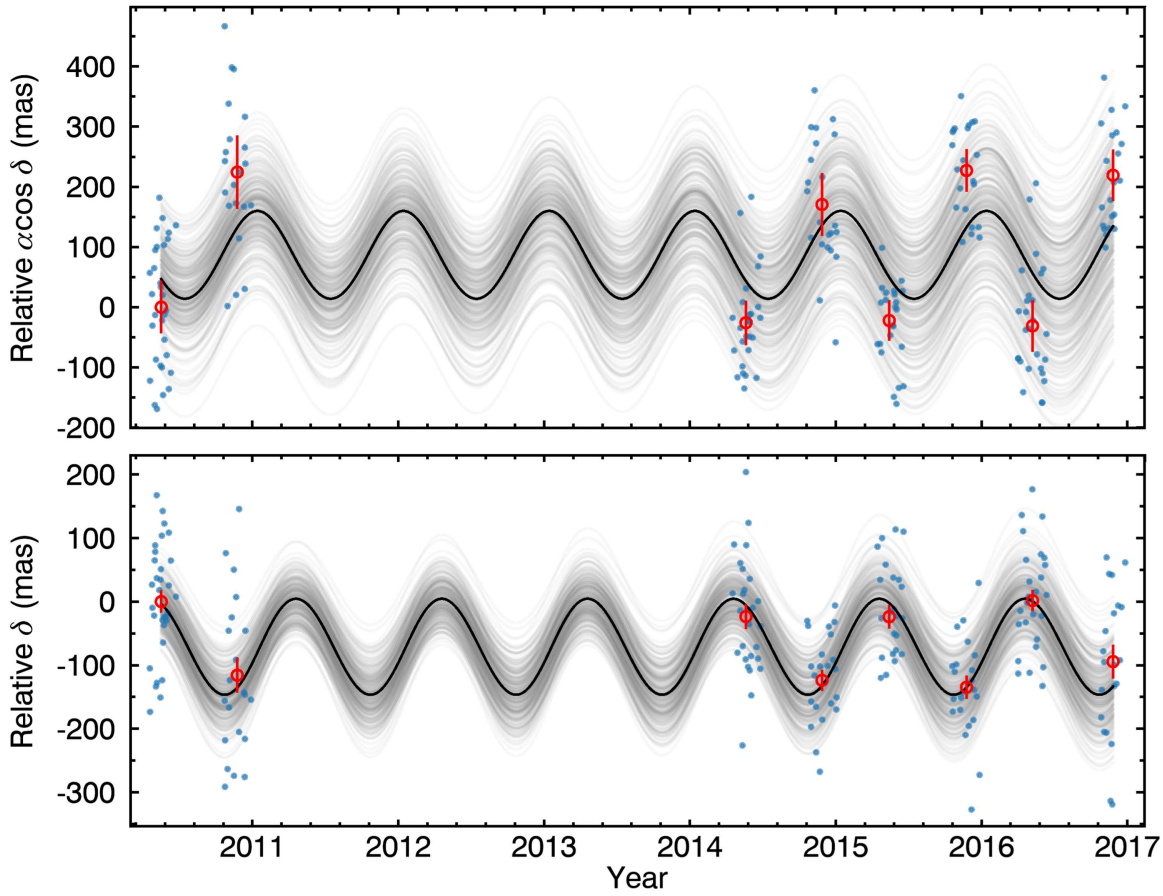

Figure 3. Relative astrometry of 2MASS J1324+6358 in right ascension and declination (red circles) with proper motion subtracted, compared to the best-fitting model (black line) and 300 random realizations selected in the Markov chains (gray lines). The blue dots are individual astrometric measurements used to build the eight astrometric epochs with the method of Theissen (2017).

of ABDMG members, corresponding to a 1.1 σ distance from the core of the BANYAN Σ model. ABDMG has a relatively large characteristic size of $\sim$19 pc in *XYZ* space (Gagné et al. 2018).

5. Fundamental Properties

5.1. Color–Magnitude Diagram

The trigonometric distance measured in Section 4.2 allows us to place 2MASS J1324+6358 in a color–magnitude diagram and compare it with the sequence of field brown dwarfs (Figure 4). 2MASS J1324+6358 falls in sequence with other young members of ABDMG, redder in $J-K$ than field brown dwarfs, and where the L/T transition takes place at a slightly fainter *J*-band magnitude. This L/T transition magnitude dependence on age was hinted by the properties of the HR 8799 bcd planets (Marois et al. 2008; Marley et al. 2012) and those of the ABDMG members SDSSp J111010.01+011613.1 and GU Psc b (Naud et al. 2014; Gagné et al. 2015a; see also the discussion of Liu et al. 2016), but 2MASS J1324+6358 provides yet stronger evidence for this effect.

5.2. Multiplicity

The fainter *J*-band magnitude of 2MASS J1324+6358 compared to the field substellar sequence goes against the spectral binary hypothesis, unless there is a large *J*-band contrast ratio between the two components, which would be inconsistent with the best-fitting L9 + T2 components identified by Looper et al. (2007) and Burgasser et al. (2010). If we assume that 2MASS J1324+6358 is an equal-mass binary with a conservative mass estimate in the range 5–60 $M_{\rm Jup}$ based on L9 + T2 spectral types at any age, our inability to resolve doubled spectral lines with the GNIRS spectrum corresponds to a weak lower limit in physical separation in the range 0.02–0.22 au, or an angular separation of $\sim$1.6–17.3 mas at the measured trigonometric distance. The absence of elongation in the point-spread function of the GNIRS acquisition images[9] puts an upper limit on the separation of an equal-luminosity binary at $\sim 0\farcs2$, or $\sim$2.5 au. The fact that the kinematics of 2MASS J1324+6358 are consistent with a membership in ABDMG is sufficient to explain its peculiar spectroscopic features, as described in Section 2. As a consequence of these considerations, we consider the binary hypothesis as highly unlikely. This is also consistent with the general picture that high variability in substellar objects seems to be correlated with low surface gravity and thus youth (Metchev et al. 2015; Gagné et al. 2017). The case of 2MASS J1324+6358 would also be reminiscent of 2MASS J21392676+0220226, which was first identified as a candidate L8.5 + T4.5 spectral binary by

[9] Available at the Gemini Science Archive at https://archive.gemini.edu.

Table 1
Properties of 2MASS J13243553+6358281

Property	Value	References
Position and Kinematics		
R.A.	13:24:45.894 ± 55 mas	1
Decl.	+63:58:12.76 ± 28 mas	1
Epoch (JD)	2455334.4 ± 0.5[a]	1
$\mu_\alpha \cos\delta$ (mas yr^{-1})	−379.7 ± 7.7	2
μ_δ (mas yr^{-1})	−66.2 ± 7.0	2
Radial velocity (km s^{-1})	$-23.7^{+0.4}_{-0.2}$	1
Parallax (mas)	78.7 ± 9.0	1
Trigonometric distance (pc)	12.7 ± 1.5	1
X (pc)	−3.5 ± 0.4	1
Y (pc)	6.9 ± 0.8	1
Z (pc)	10.1 ± 1.2	1
U (km s^{-1})	−9.5 ± 1.9	1
V (km s^{-1})	−28.8 ± 1.9	1
W (km s^{-1})	−13.6 ± 0.7	1
Photometric Properties		
i_{AB} (SDSS)	22.73 ± 0.28	3
z_{AB} (SDSS)	18.72 ± 0.04	3
J (2MASS)	15.60 ± 0.07	4
H (2MASS)	14.58 ± 0.06	4
K (2MASS)	14.06 ± 0.06	4
$W1$ (AllWISE)	13.12 ± 0.02	5
$W2$ (AllWISE)	12.29 ± 0.02	5
$W3$ (AllWISE)	10.78 ± 0.07	5
[3.6 μm] (IRAC)	12.56 ± 0.03	6
[4.5 μm] (IRAC)	12.33 ± 0.03	6
[5.8 μm] (IRAC)	11.79 ± 0.03	6
[8.0 μm] (IRAC)	11.31 ± 0.03	6
Fundamental Properties		
Spectral type	T2 ±1	6, 7
Age (Myr)	149^{+51}_{-19}	1, 8
Mass (M_{Jup})	11–12	1
Radius (R_{Jup})	1.23 ± 0.02	1
T_{eff} (K)	1080 ± 60	1
$\log g$	4.29 ± 0.02	1
$\log L_*/L_\odot$	−4.72 ± 0.10	1
Rotation period (hr)	13 ± 1	9
$v \sin i$ (km s^{-1})	$11.5^{+1.0}_{-0.8}$	1
i (°)	56^{+11}_{-7}	1

Note.
[a] This corresponds to the first combined epoch in the *WISE* measurements, where the error bar is given by the standard deviation of the individual epochs that were combined.
References. (1) This work, (2) Schneider et al. (2016a), (3) Alam et al. (2015), (4) Skrutskie et al. (2006), (5) Kirkpatrick et al. (2014), (6) Metchev et al. (2008), (7) Looper et al. (2007), (8) Bell et al. (2015), (9) Metchev et al. (2015).

Burgasser et al. (2010). Radigan et al. (2012) later ruled out the presence of a companion at separations above ∼1.6 au for a J-band contrast of 3 mag or less using *HST*/NICMOS imaging and discovered it to be highly variable with a 26% peak-to-peak J-band amplitude. This suggested that the high variability of brown dwarfs may be due to evolving and rotating patterns of patchy clouds, presenting us a combination of more than a single atmospheric layer at different effective temperatures. We can therefore suspect that highly variable brown dwarfs will cause more false positives in the detection of binaries with the spectral fitting method.

5.3. Spectral Energy Distribution

The trigonometric distance measured here was combined with the 0.8–2.5 μm low-resolution near-infrared spectrum of Looper et al. (2007) and all photometric data listed in Table 1 (i.e., SDSS, 2MASS, AllWISE, and IRAC) to build the spectral energy distribution of 2MASS J1324+6358. The method described in Filippazzo et al. (2015) and Faherty et al. (2016) was then used to directly measure its bolometric luminosity, estimate a radius and a mass based on the Saumon & Marley (2008) evolutionary models at the age of ABDMG, and translate the radius and bolometric luminosity to a semi-empirical effective temperature using the Stefan–Boltzmann law. The resulting fundamental properties of 2MASS J1324+6358 are listed in Table 1. 2MASS J1324+6358 falls in sequence with other high-likelihood ABDMG members (see Figure 4) in spectral type, mass, temperature, and $\log L_*/L_\odot$ measured with the same method (Gagné et al. 2015a; Faherty et al. 2016), although its mass estimate overlaps significantly with that of the L6–L8 γ-type bona fide member 2MASS J22443167+2043433 (Vos et al. 2018). The temperatures of 2MASS J22443167+2043433 (1180 ± 10 K; Faherty et al. 2016) and 2MASS J1324+6358 (1080 ± 60 K) provide an indication that the transition from the L to T spectral type happens at ∼1150 K at the age of ABDMG, a temperature slightly cooler than for field-aged brown dwarfs (∼1250 K; Filippazzo et al. 2015). This is consistent with previous observations in the literature (e.g., see Metchev & Hillenbrand 2006; Liu et al. 2016).

5.4. Geometric Radius Constraint

The rotation period of 2MASS J1324+6358 was measured from its *Spitzer*/IRAC light curves in the [3.5 μm] and [4.3 μm] bands by Metchev et al. (2015), who found an approximate period of 13 ± 1 hr. The probability distribution for the inclination of 2MASS J1324+6358 was explored with a Markov Chain Monte Carlo analysis based on geometry with the radius estimate and the projected rotational velocity reported in Table 1. A non-informative prior probability on the inclination $P(i) = \sin i$ was adopted. We obtain an estimate of $i = 56^{+11\circ}_{-7}$. Measurements of both the photometric period and projected rotational velocity also make it possible to derive a lower limit on the radius of 2MASS J1324+6358 that ensures $v \sin i \leqslant v$, in a model-independent way. A 10^7-elements Monte Carlo approach was performed to account for the measurement errors and yielded a lower limit of $1.22 \pm 0.2\,R_{Jup}$ on its radius, independent of evolutionary models. Comparing this limit with the Saumon & Marley (2008) models at the measured bolometric luminosity provides an upper limit of 150^{+150}_{-130} Myr on the age of 2MASS J1324+6358, independent of kinematics and consistent with membership in ABDMG.

6. Conclusions

A new trigonometric distance based on the *WISE* mission astrometry and a radial velocity measured from a GNIRS near-infrared spectrum are presented for 2MASS J1324+6358 and suggest that it is a member of the young ∼150 Myr old ABDMG. This fact alone could explain the spectroscopic peculiarities first noted by Looper et al. (2007) without the need to invoke an unresolved L9 + T2 spectral binary. The

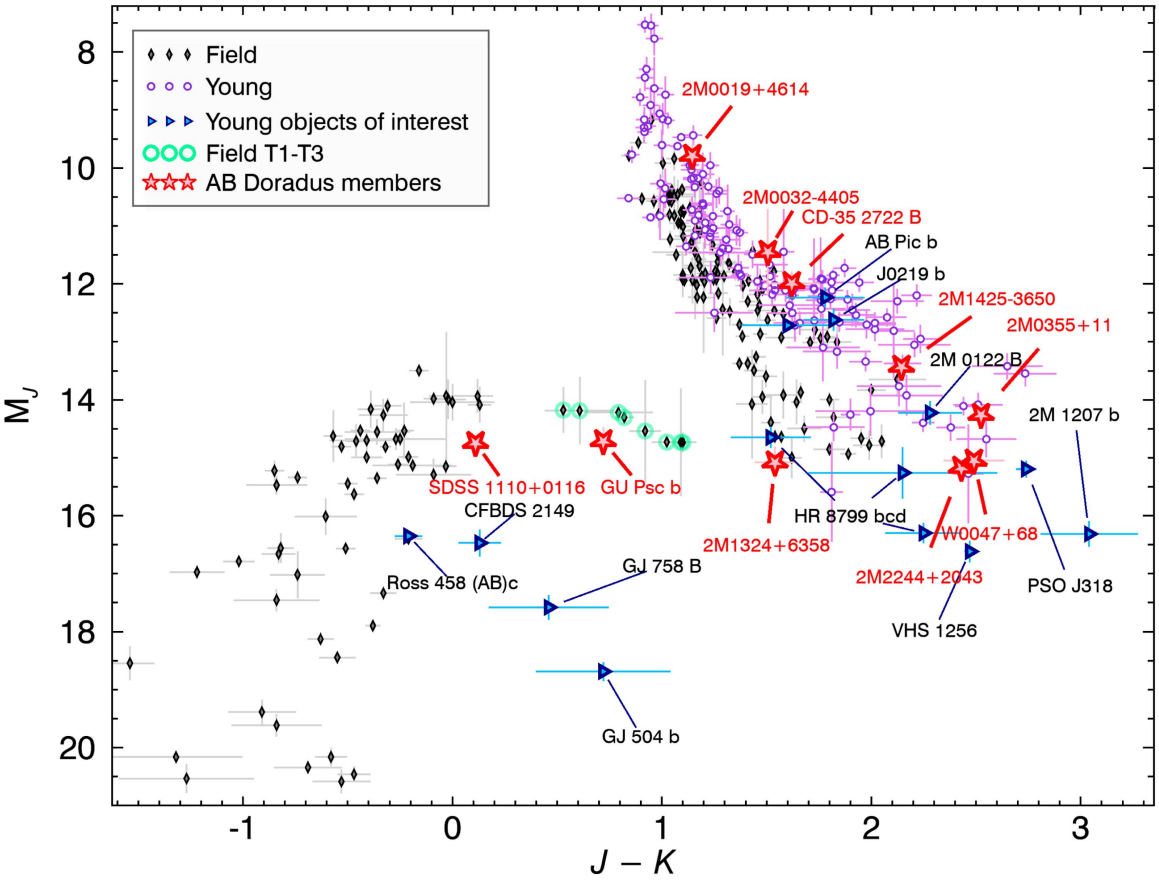

Figure 4. Color–magnitude diagram of confirmed or high-likelihood members of ABDMG (as defined by Faherty et al. 2016) with trigonometric distance measurements (red stars) compared with field (black diamonds) and young brown dwarfs (open purple circles and right-pointing blue triangles). Field brown dwarfs within one spectral subtype of 2MASS J1324+6358 are marked with a green open circle. The ABDMG members define a sequence redder than the field, with an L/T transition happening at a slightly fainter *J*-band magnitude. 2MASS J1324+6358 is both redder and fainter than field T1–T3 dwarfs in the near-infrared, similarly to young late-type L dwarfs. These data were compiled from Gagné et al. (2015b), Faherty et al. (2016), Liu et al. (2016), Vos et al. (2018), and other references therein.

trigonometric distance places 2MASS J1324+6358 in line with the sequence of other ABDMG members, at a much redder $J - K$ color than field T1–T3 dwarfs and a slightly fainter *J*-band magnitude, providing more evidence that the L/T transition at a young age happens at a fainter magnitude in this particular color–magnitude space, and at a cooler effective temperature.

We thank the anonymous referee of this Letter for a prompt and useful report. We thank Matthew Taylor, Sandy Leggett, Tom Geballe, and Lucas Fuhrman for their help with the GNIRS observing, and Jack Gallimore for his contributions to the DREAM-ZS fitting code. This research made use of data products from the Two Micron All Sky Survey (2MASS), which is a joint project of the University of Massachusetts and the Infrared Processing and Analysis Center (IPAC)/California Institute of Technology (Caltech), funded by the National Aeronautics and Space Administration (NASA) and the National Science Foundation; data products from the *Wide-field Infrared Survey Explorer* (*WISE*), which is a joint project of the University of California, Los Angeles, and the Jet Propulsion Laboratory (JPL)/Caltech, funded by NASA. Based on observations obtained at the Gemini Observatory (science program number GN-2017B-FT-21) acquired through the Gemini Observatory Archive, which is operated by the Association of Universities for Research in Astronomy, Inc., under a cooperative agreement with the NSF on behalf of the Gemini partnership: the National Science Foundation (United States), the National Research Council (Canada), CONICYT (Chile), Ministerio de Ciencia, Tecnología e Innovación Productiva (Argentina), and Ministério da Ciência, Tecnologia e Inovação (Brazil).

Software: BANYAN Σ (Gagné et al. 2018), BANYAN II (Gagné et al. 2014), emcee (Foreman-Mackey et al. 2013).

Facility: Gemini:North (GNIRS).

Note Added in Proof. Bonnefoy et al. (2016) found that the near-infrared spectrum of 2MASS J1324+6358 provides a good match to the spectral energy distribution of the young directly imaged exoplanet HR 8799 b. Furthermore, Heinze et al. (2015) find that 2MASS J1324+6358 exhibits a 20% photometric variability at optical wavelengths, and suggest that its peculiar photometric properties may be due to an inhomogeneous photosphere rather than binarity.

ORCID iDs

Jonathan Gagné https://orcid.org/0000-0002-2592-9612
Katelyn N. Allers https://orcid.org/0000-0003-0580-7244
Christopher A. Theissen https://orcid.org/0000-0002-9807-5435
Jacqueline K. Faherty https://orcid.org/0000-0001-6251-0573

Daniella Bardalez Gagliuffi https://orcid.org/0000-0001-8170-7072
Étienne Artigau https://orcid.org/0000-0003-3506-5667

References

Alam, S., Albareti, F. D., Allende Prieto, C., et al. 2015, ApJS, 219, 12
Allard, F., Homeier, D., & Freytag, B. 2012, RSPTA, 370, 2765
Allers, K. N., Gallimore, J. F., Liu, M. C., & Dupuy, T. J. 2016, ApJ, 819, 133
Allers, K. N., & Liu, M. C. 2013, ApJ, 772, 79
Bardalez Gagliuffi, D. C., Gagné, J., Faherty, J. K., & Burgasser, A. J. 2018, arXiv:1801.06134v1
Bell, C. P. M., Mamajek, E. E., & Naylor, T. 2015, MNRAS, 454, 593
Biller, B., Vos, J., Buenzli, E., et al. 2018, AJ, 155, 95
Bonnefoy, M., Zurlo, A., Baudino, J. L., et al. 2016, A&A, 587, A58
Burgasser, A. J., Cruz, K. K., Cushing, M. C., et al. 2010, ApJ, 710, 1142
Burgasser, A. J., Geballe, T. R., Leggett, S. K., Kirkpatrick, D. J., & Golimowski, D. A. 2006, ApJ, 637, 1067
Burrows, A., Hubbard, W. B., Lunine, J. I., & Liebert, J. 2001, RvMP, 73, 719
Chauvin, G., Lowrance, P., Lagrange, A.-M., et al. 2005, A&A, 438, L25
Cruz, K. L., Reid, I. N., Kirkpatrick, J. D., et al. 2007, AJ, 133, 439
Cushing, M. C., Vacca, W. D., & Rayner, J. T. 2004, PASP, 116, 362
Elias, J. H., Joyce, R. R., Liang, M., et al. 2006, Proc. SPIE, 6269, 62694C
Faherty, J. K., Riedel, A. R., Cruz, K. L., et al. 2016, ApJS, 225, 10
Filippazzo, J. C., Rice, E. L., Faherty, J., et al. 2015, ApJ, 810, 158
Foreman-Mackey, D., Hogg, D. W., Lang, D., & Goodman, J. 2013, PASP, 125, 306
Gagné, J., Burgasser, A. J., Faherty, J. K., et al. 2015a, ApJL, 808, L20
Gagné, J., Faherty, J. K., Burgasser, A. J., et al. 2017, ApJL, 841, L1
Gagné, J., Faherty, J. K., Cruz, K. L., et al. 2015b, ApJS, 219, 33
Gagné, J., Lafrenière, D., Doyon, R., Malo, L., & Artigau, É. 2014, ApJ, 783, 121
Gagné, J., Mamajek, E. E., Malo, L., et al. 2018, ApJS, in press (arXiv:1801.09051)
Gauza, B., Béjar, V. J. S., Pérez-Garrido, A., et al. 2015, ApJ, 804, 96
Heinze, A. N., Metchev, S., & Kellogg, K. 2015, ApJ, 801, 104
Kellogg, K., Metchev, S., Gagné, J., & Faherty, J. 2016, ApJL, 821, L15
Kirkpatrick, D. J., Schneider, A. C., Fajardo-Acosta, S., et al. 2014, ApJ, 783, 122
Lindegren, L., Lammers, U., Bastian, U., et al. 2016, A&A, 595, A4
Liu, M. C., Dupuy, T. J., & Allers, K. N. 2016, ApJ, 833, 96
Liu, M. C., Magnier, E. A., Deacon, N. R., et al. 2013, ApJL, 777, L20
Looper, D. L., Kirkpatrick, J. D., & Burgasser, A. J. 2007, AJ, 134, 1162
Lord, S. D. 1992, NASA Tech. Memo., 103957
Macintosh, B., Graham, J. R., Barman, T., et al. 2015, Sci, 350, 64
Malo, L., Doyon, R., Lafrenière, D., et al. 2013, ApJ, 762, 88
Naud, M.-È., Artigau, É., Malo, L., et al. 2014, ApJ, 787, 5
Marley, M. S., Saumon, D., Cushing, M., et al. 2012, ApJ, 754, 135
Marois, C., Macintosh, B., Barman, T. S., et al. 2008, Sci, 322, 1348
Metchev, S. A., Heinze, A., Apai, D., et al. 2015, ApJ, 799, 154
Metchev, S. A., & Hillenbrand, L. A. 2006, ApJ, 651, 1166
Metchev, S. A., Kirkpatrick, D. J., Berriman, G. B., & Looper, D. 2008, ApJ, 676, 1281
Naud, M.-E., Artigau, É., Rowe, J. F., et al. 2017, AJ, 154, 138
Radigan, J., Jayawardhana, R., Lafrenière, D., et al. 2012, ApJ, 750, 105
Riedel, A. R., Blunt, S. C., Lambrides, E. L., et al. 2017, AJ, 153, 95
Saumon, D., & Marley, M. S. 2008, ApJ, 689, 1327
Schneider, A. C., Greco, J., Cushing, M. C., et al. 2016a, ApJ, 817, 112
Schneider, A. C., Windsor, J., Cushing, M. C., Kirkpatrick, J. D., & Wright, E. L. 2016b, ApJL, 822, L1
Shkolnik, E. L., Allers, K. N., Kraus, A. L., Liu, M. C., & Flagg, L. 2017, AJ, 154, 69
Skrutskie, M. F., Cutri, R. M., Stiening, R., et al. 2006, AJ, 131, 1163
ter Braak, C. J. F., & Vrugt, J. A. 2008, Stat. Comput., 18, 435
Theissen, C. A. 2017, ApJ, submitted (arXiv:1710.11127)
Vos, J. M., Allers, K. N., Biller, B. A., et al. 2018, MNRAS, 474, 1041
Wright, E. L., Eisenhardt, P. R. M., Mainzer, A. K., et al. 2010, AJ, 140, 1868
Zuckerman, B., Song, I., & Bessell, M. S. 2004, ApJL, 613, L65